Available online at www.eccomasproceedia.org
Eccomas Proceedia SMART (2023) 1136-1147

ECCOMAS
Proceedia

X ECCOMAS Thematic Conference on Smart Structures and Materials
SMART 2023
D.A. Saravanos, A. Benjeddou, N. Chrysochoidis and T. Theodosiou (Eds)

MODAL SHAPE RECONSTRUCTION AND DAMAGE IDENTIFICATION OF VIBRATING PLATES USING INVERSE FINITE ELEMENT METHOD

A. KEFAL*, M. A. ABDOLLAHZADEH* AND M. Y. BELUR*

* Integrated Manufacturing Technologies Research and Application Center
Sabanci University
Tuzla, 34956, Istanbul, Turkey
e-mail: adnankefal@sabanciuniv.edu, m.abdollahzadeh1@sabanciuniv.edu,
yavuz.belur@sabanciuniv.edu

Abstract. In this study, a new structural modal model is developed based on the inverse finite element method (iFEM) to regenerate the natural frequencies and mode shapes of plates from in situ strain measurements. Also, the proposed model is applied to the structural damage diagnosis of vibrating plates. To perform the necessary simulations, a cantilever plate is analyzed with a limited number of strain gauges through the iFEM approach under hammer testing loads. To this end, the plate is dynamically simulated with/without initial damage using forward finite element analysis. The strain response at each time step is recorded as input to the iFEM analysis. The results of iFEM versus reference solutions are comprehensively compared. Consequently, the superior modal data identification and damage diagnosis capability of the proposed methodology are demonstrated. Overall, the iFEM approach has been proven as a turn-key solution for experimental modal testing and structural health monitoring of plates under vibration.

Keywords: Shape sensing; inverse finite element method; vibration; natural frequency identification; modal shape reconstruction; damage diagnosis.

1 INTRODUCTION

Plates are commonly used in different sizes and shapes to manufacture various structural components for aerospace, marine, and automotive engineering applications. Depending on the environmental/operations conditions, these structures can be subjected to a variety of dynamic loads. Therefore, performing dynamic analysis of plates is of great importance to predict the realistic mechanical response of the engineering parts. Among the class of dynamic (frequency/time/hybrid domain) analysis, experimental/numerical modal analysis serves as a vital technology in the field of structural dynamics because it enables the predictions of modal parameters, such as natural frequencies, mode shapes, and damping ratios, from simulated or measured vibration data [1-3]. This mathematical model is the modal model of the system, and the information about its properties is called “modal data”. Modal data obtained from the experiments can be utilized to perform real-time condition monitoring,

Peer-review under responsibility of the organizing committee of SMART 2023.
doi: 10.7712/150123.9863.451153

structural health monitoring, and damage diagnosis/prognosis. Hence, the development and refinement of experimental modal identification techniques are significantly required to enhance the performance and safety of a wide range of structures.

Modal testing is an experimental technique for determining the modal model of a time-invariant linear oscillatory system. The theoretical basis of this technique is based on the relationship between the vibrational response at one point in the structure and the excitation at the same or at another point as a function of excitation frequency [4]. This relationship, which often takes the form of a complex mathematical function, is called a frequency response function (FRF). In modal testing, FRFs, or the impact response of the structure, are measured. FRFs can be measured by applying a (measured) force to a point on the structure, in the absence of other excitation forces, and measuring the vibration response at one or more points on the structure. Modern excitation methods and advances in modal analysis theory have made it possible to apply more complex excitation mechanisms [5]. Experimental mode identification has various applications such as fixing bugs, matching the finite element model to the experimental results, repairing the structure, sensitivity analysis, reducing the mathematical models, and diagnosing structural defects [6-7].

For the identification of structural modes in an experiment, measurement of the frequency response can be conducted through displacement data. Thus, accurate prediction of the structural deformations in the experimental may play a critical role for full-field modal identification (e.g., natural frequencies, and model shape in three-dimensional domain). To this end, the inverse finite element method (iFEM), i.e., originally developed for the purpose of deformation reconstruction (shape sensing) from a strain sensor network [8], can be adopted to find full-field deformations of the vibrating plates in real-time. In literature, the iFEM methodology was demonstrated to be a highly accurate shape-sensing algorithm for beam/plate/shell/solid-like structures. For instance, four-node (iQS4) [9] and eight-node (iCS8) [10] inverse shell elements were developed to analyze real-time structural deformations of shell structures. According to a recent comparative and review study of the iFEM element [11], the iQS4 element became popular in the last decade for shape sensing and structural health monitoring applications [12-15].

In the study, we present a systematic iFEM/iQS4-based strategy for the first time to reconstruct structural modal data including natural frequencies and full-field structural mode shapes from the experimental strain data of the sensor network. The potential use of the present modal model based on iFEM can also be extended to damage diagnosis of vibrating plates. Therefore, after verification of the present modal system identification, a fault/damage diagnosis example is also solved using the proposed methodology. Overall, the results are compared reference solutions generated by the numerical forward analysis. Hence, the iFEM results are comprehensively validated while emphasizing the underlying principles, advantages, limitations, and practical applications of the proposed iFEM modal model. This paper is structured into four sections. After the introduction presented in Section 1, the mathematical foundation of the proposed iFEM-based modal identification method is summarized in Section 2. Lastly, Section 3 describes the numerical examples whereas the concluding remarks are provided in Section 4.

2 INVERSE FINITE ELEMENT FORMULATION

2.1 The iQS4 Element Formulation

In this study, we use a four-node quadrilateral inverse shell element, iQS4, developed originally by Kefal et al. [9]. The iQS4 element formulation is based on the Mindlin's plate kinematic relations. Accordingly, the displacement vector components of a material point within the iQS4 element can be defined as:

$$\begin{Bmatrix} u_1 \\ u_2 \\ u_z \end{Bmatrix} \equiv \begin{bmatrix} 1 & 0 & 0 & z & 0 \\ 0 & 1 & 0 & 0 & z \\ 0 & 0 & 1 & 0 & 0 \end{bmatrix} \begin{Bmatrix} u \\ v \\ w \\ \theta_1 \\ \theta_2 \end{Bmatrix} \equiv \mathbf{Z}\mathbf{u} = \mathbf{Z}\mathbf{N}^e\mathbf{u}^e \tag{1}$$

where $\mathbf{u}$ vector defines the kinematic variables of the Mindlin plate, the $\mathbf{N}^e$ matrix contains second order Lagrangian shape functions of the element [9], and the $\mathbf{u}^e$ vector defines the element degrees of freedom (DOF) vector of the iQS4 element, which is consisted of three translational and three rotational DOFs per node. Linear infinitesimal strains of any material point within the element can be calculated as:

$$\begin{Bmatrix} \varepsilon_{11} \\ \varepsilon_{22} \\ \gamma_{12} \end{Bmatrix} \equiv \begin{Bmatrix} u_{1,1} \\ u_{2,2} \\ u_{1,2}+u_{2,1} \end{Bmatrix} = \begin{Bmatrix} u_{,1} \\ v_{,2} \\ u_{,2}+v_{,1} \end{Bmatrix} + z \begin{Bmatrix} \theta_{1,1} \\ \theta_{2,2} \\ \theta_{1,2}+\theta_{2,1} \end{Bmatrix} \equiv \mathbf{e} + z\boldsymbol{\kappa} = \left(\mathbf{B}_e + z\mathbf{B}_\kappa\right)\mathbf{u}^e$$
$$\begin{Bmatrix} \gamma_{1z} \\ \gamma_{2z} \end{Bmatrix} \equiv \begin{Bmatrix} u_{1,z}+u_{z,1} \\ u_{2,z}+u_{z,2} \end{Bmatrix} = \begin{Bmatrix} w_{,1}+\theta_1 \\ w_{,2}+\theta_2 \end{Bmatrix} \equiv \boldsymbol{\gamma} = \mathbf{B}_\gamma\mathbf{u}^e \tag{2}$$

where ε_{ii} is the normal strain along x_1 and x_2 coordinates, γ_{12} is the in-plane shear strains, and γ_{iz} is the transverse (out-of-plane) shear strains of the element. These strain components are defined as first order derivatives of the kinematic variables with respect to in-plane coordinate coordinates, x_i $(i=1,2)$, which are referred to as "membrane, $\mathbf{e}$, bending, $\boldsymbol{\kappa}$, and $\boldsymbol{\gamma}$, transverse-shear section strains." Substituting the $\mathbf{N}^e\mathbf{u}^e$ approximation in these vectors and taking relevant derivatives of $\mathbf{N}^e$ with respect to in-plane coordinates, section strains are approximated using $\mathbf{B}_e$, $\mathbf{B}_\kappa$, $\mathbf{B}_\gamma$ strain-displacement relation matrices [9].

For performing an accurate iFEM analysis, a set of strain gauges or fiber optic cables should be mounted on the top and bottom of the structure within each element position. Accordingly, utilizing the in situ sensor data, the experimental membrane and bending section strains can be calculated as:

$$\mathbf{E}_i = \frac{\boldsymbol{\varepsilon}_i^+ + \boldsymbol{\varepsilon}_i^-}{2},\ \mathbf{K}_i = \frac{\boldsymbol{\varepsilon}_i^+ - \boldsymbol{\varepsilon}_i^-}{2h} \tag{3}$$

where the $\mathbf{E}_i$ and $\mathbf{K}_i$ terms are experimental counterparts of $\mathbf{e}$ and $\boldsymbol{\kappa}$ analytical section strains, respectively, and the $2h$ term stands for the total thickness of the iQS4 element.

Moreover, $\boldsymbol{\varepsilon}_i^+$ and $\boldsymbol{\varepsilon}_i^-$ vectors contain the experimental surface strain measurements obtained from the sensors at position, $\mathbf{x}_i = (x_1, x_2)_i$ $(i = 1,2,n^{sensors})$. Here, the superscripts '+' and '–' denote the top and bottom of surface of an iQS4 element, in the given order. The values of the $\mathbf{E}_i$ and $\mathbf{K}_i$ are not continues within the element as they correspond to a specific point in the element domain. Their continuous form ($\mathbf{E}_i \to \mathbf{E}$ and $\mathbf{K}_i \to \mathbf{K}$) can be obtained by employing smoothing procedures [16]. Alternatively, considering the relatively small size of each inverse element size compared to the whole structural discretization, the experimental section strain can be assumed constant over each iQS4 element. Therefore, even a single set of strain sensors is enough to obtain continuous form of the experimental section strains within the whole iFEM mesh. Note that the experimental counterpart of the $\boldsymbol{\gamma}$ section strains, represented as $\boldsymbol{\Gamma}$, can be safely omitted for the iFEM analysis of thin shell structures.

Next, to find the minimum error between analytical and experimental strains of an iQS4 element, a weighted least squares function, $\Phi^e \equiv \Phi^e(\mathbf{u}^e)$, is defined as:

$$\Phi^e = \frac{1}{A}\int_A \left(w_e \left\| \mathbf{e} - \mathbf{E} \right\|_2^2 + w_\kappa (2h)^2 \left\| \boldsymbol{\kappa} - \mathbf{K} \right\|_2^2 + w_\gamma \left\| \boldsymbol{\gamma} - \boldsymbol{\Gamma} \right\|_2^2 \right) dA \tag{4}$$

where the L_2 norms of the strain difference vectors can be computed as $\left\| \boldsymbol{\chi} \right\|_2^2 = \boldsymbol{\chi}^T \boldsymbol{\chi}$. To provide consistency between units, L_2 norm for bending curvatures is multiplied by thickness square, $(2h)^2$, and the surface integral term is normalized with the total area of the iQS4 element, A. The coefficients of w_e, w_κ, w_γ are the penalty terms, as such they are adjusted to a small positive value (i.e., compared to unity such as $\lambda = 10^{-4}$) for the iQS4 elements without sensors. Otherwise, they are set to unit number 1 for elements with a sensor. To solve an iFEM problem, first variation of the Eq. (4) with respect to $\mathbf{u}^e$ can be performed as:

$$\delta\Phi^e = \frac{2}{A}\int_A \left(w_e \delta\mathbf{e}^T (\mathbf{e} - \mathbf{E}) + w_\kappa (2h)^2 \delta\boldsymbol{\kappa}^T (\boldsymbol{\kappa} - \mathbf{K}) + w_\gamma \delta\boldsymbol{\gamma}^T (\boldsymbol{\gamma} - \boldsymbol{\Gamma}) \right) dA + \delta\varphi_0 \tag{5}$$

where the variation of the experimental measurements vanishes, $\delta\varphi_0 = 0$. Analytical section strains given in Eq. (2) can be substituted into the Eq. (5), and the resultant can be minimized to obtain the final set of iFEM equations as:

$$\delta\Phi^e = \delta\mathbf{u}^{eT} \left(\mathbf{k}^e \mathbf{u}^e - \mathbf{f}^e \right) = 0 \to \mathbf{k}^e \mathbf{u}^e = \mathbf{f}^e \tag{6}$$

where $\mathbf{k}^e$ and $\mathbf{f}^e$ are the shape (left-hand-side) matrix and experimental-strain-data (right-hand-side) vectors, respectively. These quantities constitute the iQS4 equations as:

$$\mathbf{k}^e = \frac{1}{A}\int_A \left(w_e \mathbf{B}_e{}^T \mathbf{B}_e + w_\kappa (2h)^2 \mathbf{B}_\kappa{}^T \mathbf{B}_\kappa + w_\gamma \mathbf{B}_\gamma{}^T \mathbf{B}_\gamma \right) dA \tag{7}$$

$$\mathbf{f}^e = \frac{1}{A}\int_A \left(w_e \mathbf{B}_e{}^T \mathbf{E} + w_\kappa (2h)^2 \mathbf{B}_\kappa{}^T \mathbf{K} + w_\gamma \mathbf{B}_\gamma{}^T \boldsymbol{\Gamma} \right) dA$$

The local equations must be transformed to a global form by considering basis vectors of elemental and global coordinate systems of the structural domain. Note that this transformation can be performed like the classical finite element analysis. Then, the global

equations of each iQS4 element can be assembled to obtain a global equation system of the entire discretization. Afterwards, constraint boundary conditions are applied to solve the global system, and subsequently obtain displacement DOF in the full-field domain.

2.2 Structural Modal Model and Damage Diagnosis

The iFEM/iQS4 analysis produces the full-field displacement DOF of the structure, these displacements can be post processed into meaningful data for various applications as well. Here, modal shape and damage identification are concurrently investigated. Since iFEM produces responses in time domain, these responses need to be switched to frequency domain. This can be done with Fourier transformation of the real-time response. There are different algorithms readily available to achieve fast and reliable Fourier transformation of the signal. One such method is Fast Fourier Transformation that finds the frequency spectrum of the signal in $O(N \log N)$ time where N is the length of the sequence. In general, FFT is achieved by separating the even and odd terms of the Discrete Fourier Transformation (DFT) from each other. In the complex mathematical form, the DFT sequence can be written as:

$$A_k = \sum_{n=0}^{N-1} a_n e^{-\frac{2\pi i}{N} nk} \quad (k = 1, 2....., N-1) \tag{8}$$

where, a_n is the value of the signal in discrete time samples. Moreover, the sequence given in Eq. (8) can be separated into even and odd terms by using the Cooley-Tukey algorithm. For the brevity, details of these algorithms are not included here.

The FFT analysis provides useful quantities in the frequency domain to obtain meaningful data that simply cannot be deducted from the time domain signal. One such usage of the FFT is for obtaining frequency response functions (FRFs). Since the iFEM output data in time domain is available in the full-field domain, the reconstructed displacement data can be switched into frequency domain by FFT, and then FRFs can be obtained by sampling response data for a range of frequencies on any point on the structure regardless of the sensor locations. Then, examining the peaks in FRFs of displacements at different locations of the structural domain, natural frequencies of the structure can be obtained. Plotting the magnitudes of the FRFs over the full-field structural domain for each natural frequency, one can inspect the contour plots of the structural mode shapes. Correct identification of the structural modal data lends itself to accurate damage identification because the natural frequencies of the pristine and damaged structures are expected to be different, and thus can be effectively compared for each time series of strain data acquisition using iFEM-FRFs data. Hence, it is possible to diagnose the damage by observing the shift in the locations of the natural frequency peaks between pristine and damaged configurations.

3 NUMERICAL EXAMPLES

In this section, the iFEM-based model identification and damage diagnosis procedures described in Section 2 are verified by performing modal testing of a cantilever plate. To this end, pristine and damaged cases of a plate subjected to an instantaneous impact, namely “hammer test”, is considered as depicted in Figure 1. Hammer test is simulated by running

full transient analysis based on forward finite element method (FEM) in Ansys Mechanical APDL software. During the simulation, physical damping is set to zero; however, a small numerical damping (which is less than 1%) is enforced by default in the transient solution stage of Ansys. Moreover, Newmark integration scheme is utilized to solve the transient problem. To create virtual discrete strain data for iFEM analysis, the strain data is exported for different sampling frequencies, namely 0.5 kHz and 1 kHz. Note that these forward analyses are not required for an experimental test given that strain data can be collected directly from the strain gauges in real time. It is worth noting that sampling frequency is identical to integration frequency of the forward transient analysis. Hereafter, terminology of "strain sampling frequency" is adopted to be consisted with the experimental terminology for strain sensors. In addition to transient analysis, modal analysis of both pristine and damaged case is performed to obtain natural frequencies of the structure. These modal analysis results can be considered as a reference solution for the iFEM analyses. Then, these reference results compared with the iFEM mode identification results to show the high accuracy of the presented method.

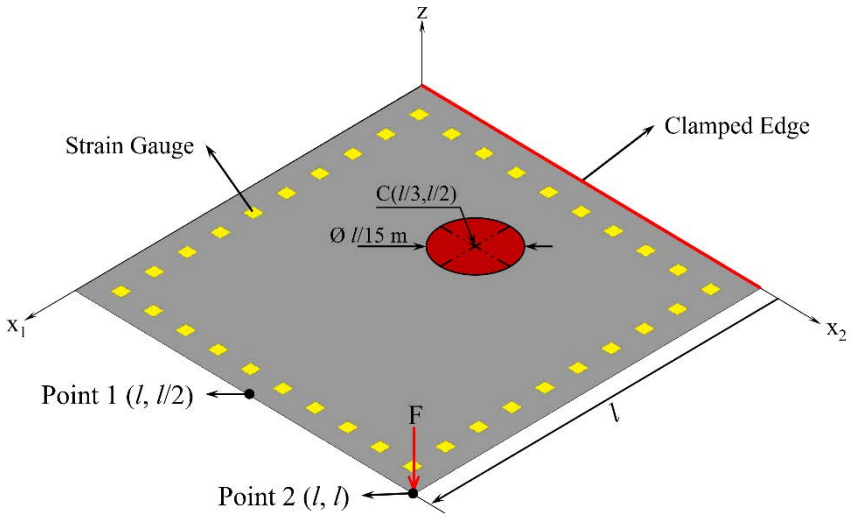

Figure 1: Plate geometry, damage shape and position, applied load and iFEM sensor placement model.

The square plate shown in Figure 1 is subjected to an impact load of F = 1 N, which is applied at $(x_1, x_2) = (1,1)$ in the negative z direction at onset of the transient analysis for about 0.002 s. One edge of the plate is fully clamped so all the kinematic variables along the clamped edge are constrained. The plate has a length of l = 1 m and a thickness of $2h$ = 5 mm. As presented in Figure 1, circular damage location and size are introduced as a parameter of the length. The plate is made of an isotropic material with elastic modulus of 200 GPa, Poisson ratio of 0.3 and density of 7850 kg/m^3. To simulate the damage accurately, the elastic modulus of the finite elements encountered in the damaged region is degraded by a factor of 10^{-5}. Here, 36 strain sensors are placed in a square array parallel to plate edges. This number

of strain gauges can be minimized by applying smoothing element analysis [16]. Nevertheless, our aim is to verify the capability of the proposed approach for the present scenario; therefore, the present number of sensors is not the main concern. For the forward finite element analysis, the discretization of the model has 30×30 shell elements both for pristine and damaged cases. On the other hand, 10×10 uniformly distributed iQS4 elements are utilized to conduct iFEM analysis. Note that in the iFEM analysis, elements with sensors have weighting coefficients of unity whereas the elements without sensors are assigned to weighting coefficients of 10^{-4}. After performing iFEM and FEM (reference) simulations, the transient displacement response at $(x_1, x_2) = (1, 0.5)$, named as Point 1, is plotted in Figure 2. In this figure, iFEM results and reference solution almost identically match each other for different time steps. Therefore, this result verifies the high shape-sensing capability of the iQS4 element for real-time monitoring of vibrating plates.

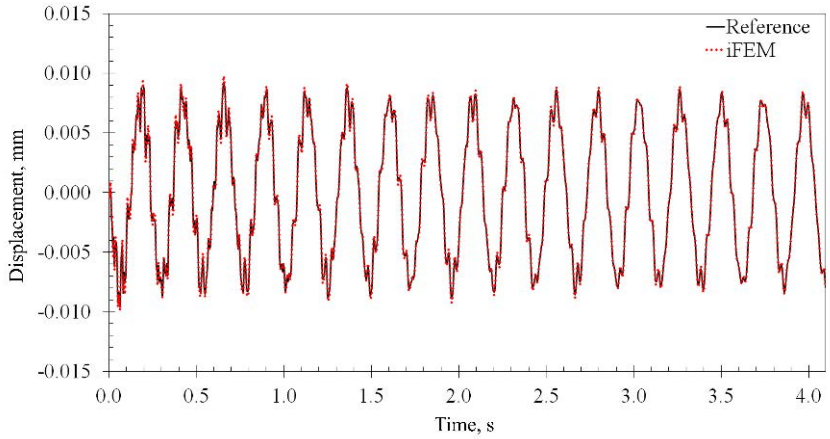

Figure 2: Displacements response at Point 1 obtained from reference solution and iFEM analysis for strain sampling frequency of 0.5 kHz.

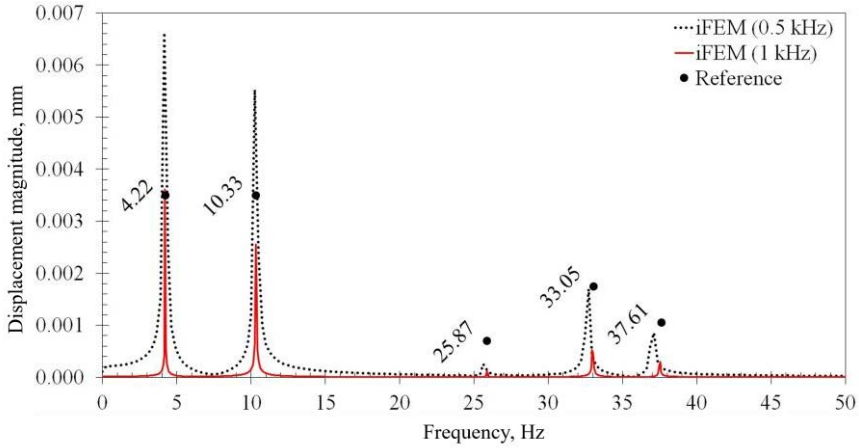

Figure 3: Comparison of reference (natural) frequencies of the plate and FRF of displacements at Point 2 obtained from iFEM for 0.5 kHz and 1 kHz strain sampling frequencies.

The iFEM response in time domain is then switched to frequency domain, and natural frequencies are identified by the modal shape reconstruction methodology presented in Section 2.2. To inspect the FRF results, displacement response of any point within plate domain can be selected. This is true for a real experiment of the present hammer test case as well since the displacement field of the entire domain is available from the iFEM solution. Therefore, there is no need to select measurement points prior to the experiment for mode identification using iFEM. Thus, after iFEM analysis, we plot the displacement FRF at Point 2, $(x_1, x_2) = (1,1)$ to identify the natural frequencies of the plate as shown in Figure 3. In this figure, iFEM (0.5 kHz) and iFEM (1 kHz) solutions correspond to the iFEM analyses performed by using the strain data input sampled at 0.5 kHz and 1 kHz, respectively. Also, the modes found from the reference modal analysis (i.e., obtained from FEM) are marked in Figure 3 as black dots with the corresponding natural frequencies next to them. For the bandwidth of 50 Hz, FRF peaks of iFEM (0.5 kHz) and iFEM (1 kHz) results precisely coincide with reference natural frequencies of the plate. On the other hand, the precision of iFEM (0.5 Hz) slightly diminishes at the higher frequencies whereas iFEM analysis with 1 kHz sampled strain-sensor data still provides excellent accuracy. Such a result is expected since lower sampling frequencies results in a lower resolution of the FFT simulation.

Table 1: Pristine modes and percent difference (PD) with respect to modal analysis results.

Mode	Reference Freq., Hz	iFEM (0.5 kHz) Prediction, Hz	iFEM (1kHz) Prediction, Hz	PD for iFEM (0.5 kHz), %	PD for iFEM (1 kHz), %
1	4.22	4.15	4.21	1.6	0.2
2	10.33	10.25	10.31	0.8	0.2
3	25.87	25.63	25.88	0.9	0.03
4	33.05	32.71	33.02	1.0	0.1
5	37.61	37.11	37.48	1.3	0.3
6	65.81	62.50	65.06	5.0	1.1
7	74.46	70.31	73.67	5.6	1.1
8	77.95	73.24	76.90	6.0	1.3
9	86.24	79.59	84.78	7.7	1.7

To elaborate on this, the first nine different modes of the plate predicted by iFEM (0.5 kHz) and iFEM (1 kHz) are listed in Table 1. As can be seen from the percent differences between iFEM results and reference solutions, iFEM (0.5 kHz) analysis produces up to 7.7% error for the natural frequency identification while iFEM (1 kHz) can precisely identify the first 9 modal frequencies of the plate with errors less than 1.7%. However, the results of iFEM (0.5 kHz) up to 5^{th} mode are precise enough since the 0.5 kHz sampling frequency is nearly adequate for the 0-35 Hz bandwidth. Furthermore, modal shapes reconstructed by iFEM (1 kHz) analysis are compared with the reference FEM solution in Figure 4. As can be seen from this figure, the iFEM displacement contours are almost indistinguishable from the reference solution, thereby confirming the excellent capabilities of the iFEM/iQS4 methodology for full-field mode shape reconstruction of vibrating plates.

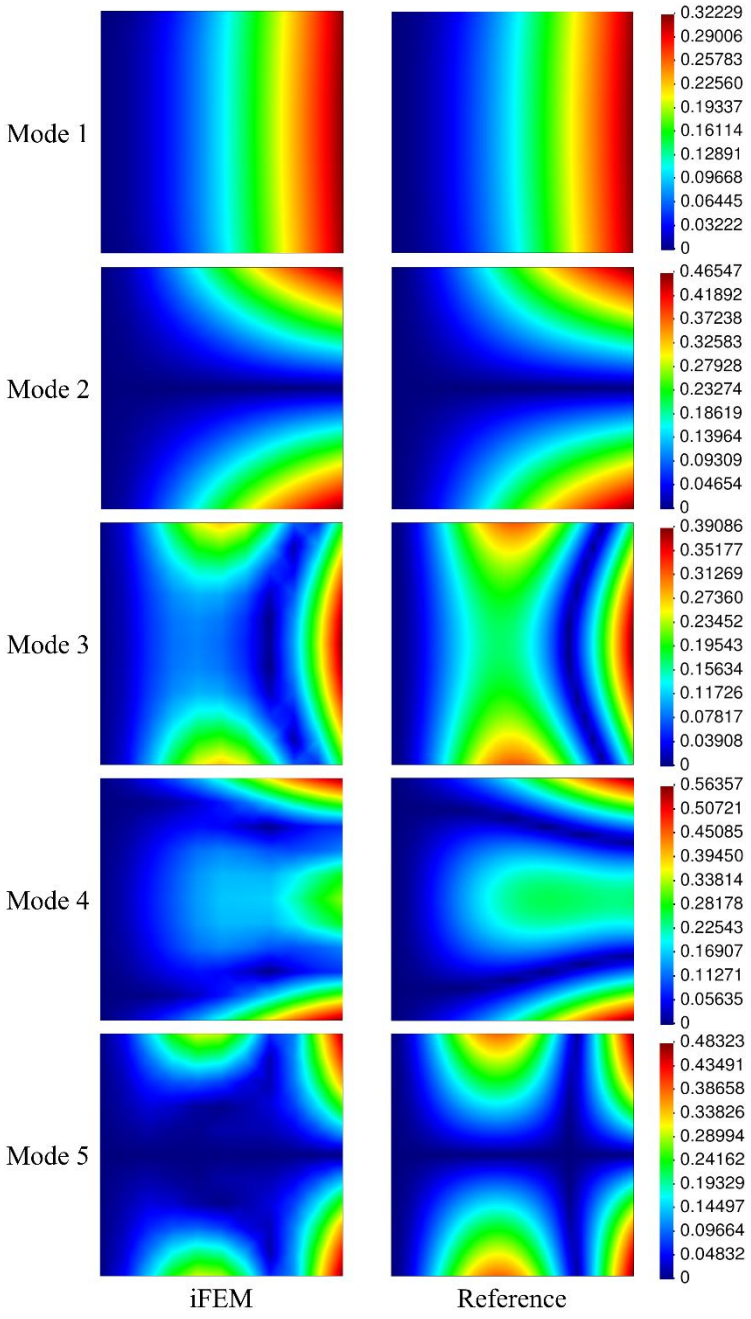

Figure 4: Comparison of iFEM (1 kHz) and reference solution contours for the mode shapes of the plate.

The damage diagnosis capability of the proposed inverse method can be explored by conducting an iFEM analysis with the strain data (e.g., the sampling rate of 1 kHz) acquired from sensors mounted on the damaged plate. In Figure 5, the real-time deformations at Point 1 obtained from iFEM analysis are plotted to illustrate the difference of the structural

response between pristine and damaged plate. According to the time-domain response in this figure, one can obviously observe that the iFEM displacement solution includes the effect of the damage introduced to the plate model. Then, for diagnosing the damage more carefully, displacement FRF responses obtained from iFEM analysis for pristine and damaged conditions of the plate are compared in Figure 6. Here, the first 5 peaks of the displacement FRF shift to lower modal frequencies, which can be attributed to the presence of damage available in the interior domain. Besides, the frequencies readings of iFEM for the damaged case are almost identical to the reference natural frequencies of the damaged plate. Hence, it is confirmed that the proposed iFEM/iQS4 methodology provides high accuracy for both time and frequency response for the damaged case as well. Also, it enables the correct identification of major modes in the damaged plate, thus serving as a promising tool for damage diagnosis of vibrating plates.

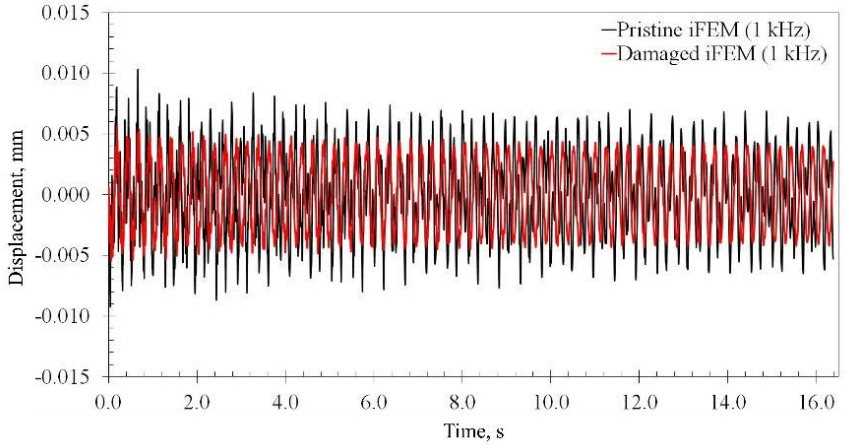

Figure 5: Pristine and damaged structures displacement response at Point 1.

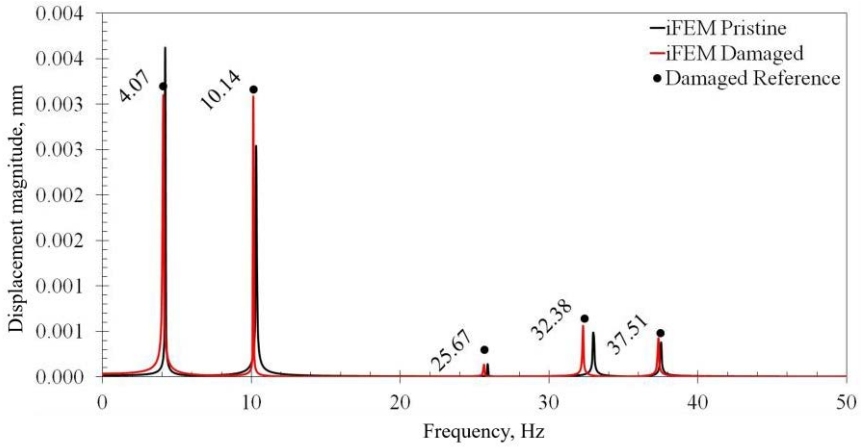

Figure 6: Comparison of displacement FRF at Point 2 obtained from iFEM simulations of damaged and pristine plates as well as reference (natural) frequencies of the damaged plate.

4 CONCLUDING REMARKS

In this research effort, the accuracy of the iFEM/iQS4 element formulation is explored for modal shape reconstruction and natural frequency identification by conducting a numerical simulation of a hammer tests on a cantilever plate. Two different hammer tests simulation are performed with different strain sampling frequencies. In addition, a circular damage is introduced to pristine model and a high frequency hammer test is simulated to verify the precision of the method for the damaged case as well. Performing iFEM analysis with different strain-data sampling as input, modal shapes of a plate under low-frequency vibration are correctly reconstructed. Moreover, it is demonstrated that the precision of the iFEM/iQS4 method increases with higher strain sampling frequency. Furthermore, even though it is possible to obtain natural frequencies just by directly utilizing a single measurement location reading, the suggested iFEM based approach is a post processing extension of the full field displacement solution of the iFEM. Therefore, it is shown in addition to precise natural frequency prediction of the method, iFEM can reconstruct full-field mode shape of the structure for a given natural frequency by using just a limited number of sensors.

Although the results of the 0.5 kHz strain sampling rate accurately predict the low natural frequencies well, higher sampling frequencies, e.g., 1 kHz, increase the precision of the iFEM methodology exponentially. As such, it is demonstrated that iFEM can determine the first 9 natural frequencies of the plate with less than 2% error. Furthermore, the damaged case results of the iFEM analysis confirm precise damage diagnosis capability of the proposed method. Therefore, it can be concluded that the proposed iFEM strategy is a promising method for constructing a structural modal model (natural frequency identification and modal shape reconstruction) as well as performing structural health monitoring of vibrating plates. Further research should focus on the experimental verification of the numerical results for both intact and damaged structures. Besides, new sensor placement models can be explored for modal testing in future studies by taking advantage of the smoothed iFEM formulation [16] for a sensor network with a small number of strain gauges and/or fiber optic sensing.

REFERENCES

[1] E. Hinton, *Numerical methods and software for dynamic analysis of plates and shells*. Pineridge Press, 1988.

[2] W. Heylen, S. Lammens, and P. Sas, *Modal analysis theory and testing* (no. 7). Katholieke Universiteit Leuven Leuven, Belgium, 1997.

[3] P. Avitabile, "Experimental modal analysis," *Sound and vibration,* vol. 35, no. 1, pp. 20-31, 2001.

[4] D. L. Brown and R. J. Allemang, "The modern era of experimental modal analysis," *Sound and Vibration,* vol. 41, no. 1, pp. 16-33, 2007.

[5] N. Maia and J. Silva, "Modal analysis identification techniques," *Philosophical Transactions of the Royal Society of London. Series A: Mathematical, Physical and Engineering Sciences,* vol. 359, no. 1778, pp. 29-40, 2001.

[6] C. Ligang, M. Shiming, Z. Yongsheng, L. Zhifeng, and Y. Wentong, "Finite element modeling and modal analysis of heavy-duty mechanical spindle under multiple constraints," *Journal of Mechanical engineering,* vol. 48, no. 3, pp. 165-173, 2012.

[7] A. Cusano *et al.*, "Experimental modal analysis of an aircraft model wing by embedded fiber Bragg grating sensors," *IEEE Sensors Journal,* vol. 6, no. 1, pp. 67-77, 2006.

[8] A. Tessler and J. L. Spangler, "A least-squares variational method for full-field reconstruction of elastic deformations in shear-deformable plates and shells," *Computer methods in applied mechanics and engineering,* vol. 194, no. 2-5, pp. 327-339, 2005.

[9] A. Kefal, E. Oterkus, A. Tessler, and J. L. Spangler, "A quadrilateral inverse-shell element with drilling degrees of freedom for shape sensing and structural health monitoring," *Engineering science and technology, an international journal,* vol. 19, no. 3, pp. 1299-1313, 2016.

[10] A. Kefal, "An efficient curved inverse-shell element for shape sensing and structural health monitoring of cylindrical marine structures," *Ocean Engineering,* vol. 188, p. 106262, 2019.

[11] M. A. Abdollahzadeh, A. Kefal, and M. Yildiz, "A comparative and review study on shape and stress sensing of flat/curved shell geometries using C0-continuous family of iFEM elements," *Sensors,* vol. 20, no. 14, p. 3808, 2020.

[12] M. Esposito and M. Gherlone, "Composite wing box deformed-shape reconstruction based on measured strains: Optimization and comparison of existing approaches," *Aerospace Science and Technology,* vol. 99, p. 105758, 2020.

[13] A. Kefal and E. Oterkus, "Displacement and stress monitoring of a Panamax containership using inverse finite element method," *Ocean Engineering,* vol. 119, pp. 16-29, 2016.

[14] L. Colombo, D. Oboe, C. Sbarufatti, F. Cadini, S. Russo, and M. Giglio, "Shape sensing and damage identification with iFEM on a composite structure subjected to impact damage and non-trivial boundary conditions," *Mechanical Systems and Signal Processing,* vol. 148, p. 107163, 2021.

[15] A. Kefal, C. Diyaroglu, M. Yildiz, and E. Oterkus, "Coupling of peridynamics and inverse finite element method for shape sensing and crack propagation monitoring of plate structures," *Computer Methods in Applied Mechanics and Engineering,* vol. 391, p. 114520, 2022.

[16] A. Kefal, I. E. Tabrizi, M. Yildiz, and A. Tessler, "A smoothed iFEM approach for efficient shape-sensing applications: Numerical and experimental validation on composite structures," *Mechanical Systems and Signal Processing,* vol. 152, p. 107486, 2021.